Magnetometric problem for a 2-D body of polygonal cross-section buried in the unbounded magnetic halfspace

M. Hvoždara, A. Kaplíková
Geophysical Institute of the Slovak Academy of Sciences[1]

A b s t r a c t: We present the exact boundary integral formulae for calculation of the magnetic anomaly due to a two dimensional body whose permeability is μ_T and its cross-section is bounded by the closed general polygonal contour. This body is buried in a wide-spreaded halfspace (e.g. lava field) of magnetic permeability μ_1. The upper halfspace is non-magnetic, its permeability is μ_0. The boundary integral technique for this problem requires the application of two-term logarithmic potential. Numerical calculations on the basis of derived formulae revealed that the surface anomaly ΔT reflects the "topography" mainly of the upper boundary of the perturbing body. The derived algorithm and numerical program enables the calculation of a lot of interesting models: magnetic intrusions, polygonal valleys, polygonal mine galleries, etc.

Key words: magnetometric models, the boundary integral technique, magnetometric profile measurements

1. Formulation and the B. I. E. solution

Solution of the forward magnetometric problem for two or three dimensional isolated bodies belongs to the "classical geophysics", e.g. *Grant and West (1965); Logachev and Zacharov (1979).* The exact analytical solutions by means of separation of variables in Laplace's or Poisson's equations were performed for "smooth bodies": sphere, cylinder, ellipsoid, using the separability of these partial differential equations *(Moon and Spencer, 1971).* If the body is of more general shape (e.g. polyhedron), the solution is performed on the basis of Poisson theorem by the assumption of uniform magnetization inside the body. More detailed analyses revealed that the uniform magnetization holds true only for bodies, which are bounded by

[1] Dúbravská cesta 9, 845 28 Bratislava, Slovak Republic; e-mail: geofhvoz@savba.sk

a smooth, quadratic surfaces (sphere, cylinder, ellipsoidal cylinder). There was revealed that the uniformity of magnetization is violated mainly near the corners of polyhedral bodies. The exact solution for polyhedral bodies can be performed using the methods of finite differences, finite elements or boundary equations. The last method mentioned seems to be more effective in comparison to the previous two, since the numerical calculations are concentrated mainly to the boundary surface.

The theory of boundary integral calculations of magnetometric anomalies due to 3D and 2D bodies bounded by a piecewise smooth (Lyapunov's) surface S and situated in unbounded nonmagnetic medium was presented in the earlier paper *(Hvoždara, 1983)*. There was done also a quite satisfactory comparison with a classical method based on the Poisson's theorem. We generalize the presented analysis to more complicated case, when the 2D body of permeability μ_T, bounded by a polygon L is buried in the halfspace "1" $z \geq 0$ of permeability μ_1 and the upper halfspace "0", $z < 0$ is nonmagnetic, so its permeability is $\mu_0 = 4\pi \times 10^{-7}$ Henry/m. This model is the shape generalization of the previous case, which was solved analytically in bipolar co-ordinates for the circular cylinder *(Hvoždara and Kaplíková, 2005)*.

In the presented paper we suppose that the 2D body is bounded by the closed polygon with $N+1$ vertices in the plane (x, z), see Fig. 1. We denote the vertices as $A_k, k = 1, 2, \ldots, N+1$, where $N \geq 3$ and the first vertex A_1 is identical with the last one $A_{N+1} \equiv A_1$. These vertices are connected by the line segments T_k, their number is N and the lengths are T_k:

$$T_k = \left[(x_{k+1} - x_k)^2 + (z_{k+1} - z_k)^2\right]^{1/2}. \tag{1}$$

The theory of stationary magnetic field *(Stratton, 1941)* enables us to calculate the magnetic field by means of magnetic potential $U(x, z)$:

$$\boldsymbol{H} = -\operatorname{grad} U. \tag{2}$$

The unperturbed magnetic field potential in the upper halfspace is as

$$V_0(x, z) = -H_0(x \cos\alpha + z \sin\alpha), \tag{3}$$

where $H_0 = |\boldsymbol{B}_0|/\mu_0$ is its intensity and $\boldsymbol{B}_0$ is the induction vector of ambient geomagnetic field (unperturbed), its absolute value is B_0, for Slovak

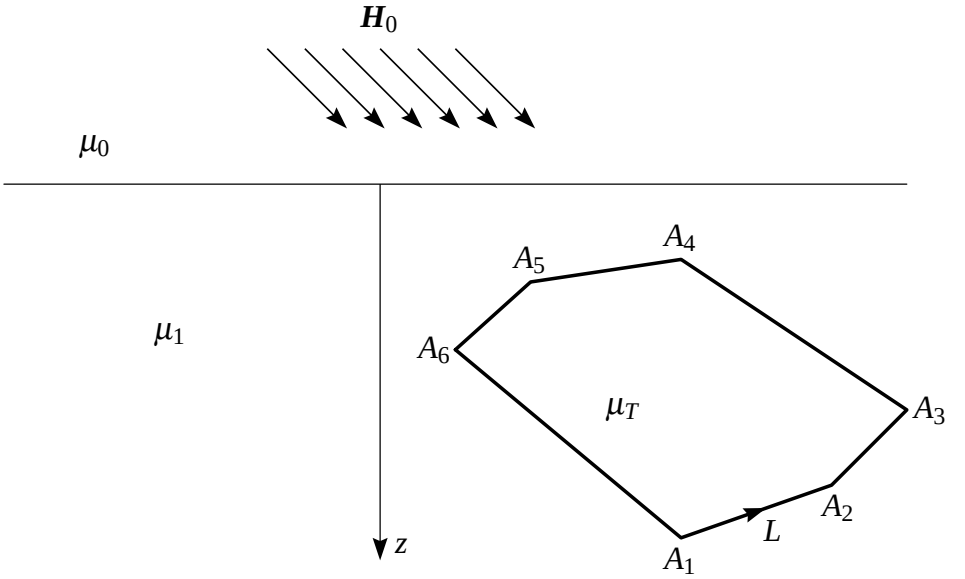

Fig. 1. Scheme for the two dimensional perturbing body embedded in the magnetic halfspace with oblique ambient magnetic field B_0.

territory about 47 000 nanoTeslas (nT) and α is the inclination angle. The deeper generalization of our treatment given in *Hvoždara (1983)* for simpler case (magnetic body in non-magnetic ambient medium) now leads to the formulae of potentials in three media as follows:

$$U_0(\boldsymbol{r}) = V_0(\boldsymbol{r}) + \frac{1}{2\pi} \int\limits_L f(\boldsymbol{r}') \frac{\partial}{\partial n'} g_0(\boldsymbol{r}, \boldsymbol{r}') \, \mathrm{d}\ell', \quad P(\boldsymbol{r}) \in \text{“0”}. \tag{4a}$$

$$U_1(\boldsymbol{r}) = V_1(\boldsymbol{r}) + \frac{1}{2\pi} \int\limits_L f(\boldsymbol{r}') \frac{\partial}{\partial n'} g_1(\boldsymbol{r}, \boldsymbol{r}') \, \mathrm{d}\ell', \quad P(\boldsymbol{r}) \in \text{“1”}. \tag{4b}$$

$$U_T(\boldsymbol{r}) = \frac{\mu_1}{\mu_T} \left\{ V_1(\boldsymbol{r}) - v_0 + \frac{1}{2\pi} \int\limits_L f(\boldsymbol{r}') \frac{\partial}{\partial n'} g_1(\boldsymbol{r}, \boldsymbol{r}') \, \mathrm{d}\ell' \right\} +$$

$$+ (1 - \mu_1/\mu_T) v_0, \qquad P(\boldsymbol{r}) \in \mathrm{Int}(L), \tag{4c}$$

where v_0 is the mean value of exciting potential $V_1(\boldsymbol{r})$ on the boundary contour L:

$$v_0 = \frac{1}{|L|} \int_L V_1(\boldsymbol{r}) \, \mathrm{d}\, \ell. \tag{5}$$

In formulae (4a)–(4c) the calculation point $\boldsymbol{r} \equiv (x, z)$ is outside L and the point $\boldsymbol{r}' \equiv (x', z')$ lies on the L, it is the running integration point. The unperturbed potential is given by (3) and its continuation inside "1" is:

$$V_1(\boldsymbol{r}) = V_1(x, z) = -xH_{0x} - z\, D\, H_{0z}, \tag{6}$$

where $D = \mu_0/\mu_1$ as was derived in *(Hvoždara and Kaplíková, 2005)*. The function $f(\boldsymbol{r})$, which occurs in (4a–c) is the modified double layer density distributed along the curve L, which is simply related to the potential $U_T(\boldsymbol{r})$ on L:

$$f(\boldsymbol{r}) = (1 - \mu_1/\mu_T) U_T(\boldsymbol{r}) + v_0, \qquad P(\boldsymbol{r}) \in L. \tag{7}$$

This density must be calculated by means of the boundary integral equation (B. I. E.):

$$f(\boldsymbol{r}) = 2\beta \left[V_1(\boldsymbol{r}) - v_0 \right] + \frac{\beta}{\pi} \backslash\!\!\!\int_L f(\boldsymbol{r}') \frac{\partial}{\partial n'} g_1(\boldsymbol{r}, \boldsymbol{r}') \, \mathrm{d}\, \ell',$$

$$\beta = (1 - \mu_T/\mu_1)/(1 + \mu_T/\mu_1), \qquad P(\boldsymbol{r}) \in L. \tag{8}$$

The backslash on the integral in (8) denotes the integration in the principal value sense.

2. Greens functions of our problem

In formulae given above, there occur normal derivatives of Green's functions $g_0(\boldsymbol{r}, \boldsymbol{r}')$, $g_1(\boldsymbol{r}, \boldsymbol{r}')$. In what follows the basic singular part in these functions is logarithm of expression $|\boldsymbol{r} - \boldsymbol{r}'|^{-1} = [(x - x')^2 + (z - z')^2]^{-1/2}$. Its normal derivative is calculated by means of formula:

$$\frac{\partial}{\partial n'} \ln |\boldsymbol{r} - \boldsymbol{r}'|^{-1} = \frac{\boldsymbol{n}' \cdot (\boldsymbol{r} - \boldsymbol{r}')}{|\boldsymbol{r} - \boldsymbol{r}'|^2} = \frac{n'_x \cdot (x - x') + n'_z \cdot (z - z')}{|\boldsymbol{r} - \boldsymbol{r}'|^2}, \tag{9}$$

where $\boldsymbol{n}' \equiv (n'_x, n'_z)$ is outer normal on the contour line L, which is in our case composed of N segments T_k. The function $g_0(\boldsymbol{r}, \boldsymbol{r}')$ relates to the halfspace "0", where it satisfies Laplace equation, the function $g_1(\boldsymbol{r}, \boldsymbol{r}')$ in lower halfspace satisfies Poisson equation, because there is situated the perturbing body "2". On the boundary $z = 0$ there are prescribed boundary conditions corresponding to potentials of magnetic intensity. Then we have to solve known two-dimensional equations:

$$\nabla^2 g_0(\boldsymbol{r}, \boldsymbol{r}') = 0, \tag{10}$$

$$\nabla^2 g_1(\boldsymbol{r}, \boldsymbol{r}') = -2\pi\delta(x - x')\delta(z - z'), \tag{11}$$

where $\nabla^2 \equiv \partial^2/\partial x^2 + \partial^2/\partial z^2$ is 2D Laplace operator. The boundary conditions on plane $z = 0$ are:

$$g_0|_{z=0} = g_1|_{z=0}\,, \tag{12}$$

$$[\partial g_0/\partial z]_{z=0} = (\mu_1/\mu_0)\,[\partial g_1/\partial z]_{z=0}\,. \tag{13}$$

In the Poisson equation (11) we have on the right side the two-dimensional Dirac's function $\delta(\boldsymbol{r} - \boldsymbol{r}') = \delta(x - x')\delta(z - z')$, where the point of singularity (x', z') is on the boundary line L of the perturbing body. The theory of classical potential shows that this singularity holds true for potential of y-directed line source:

$$\ln |\boldsymbol{r} - \boldsymbol{r}'|^{-1} = \ln \left[(x - x')^2 + (z - z')^2\right]^{-1/2}, \tag{14}$$

as a fundamental solution of 2D Poisson equation

$$\nabla^2 \ln |\boldsymbol{r} - \boldsymbol{r}'|^{-1} = -2\pi\delta(\boldsymbol{r} - \boldsymbol{r}'). \tag{15}$$

Hence, this logarithmic potential is the basic part of $g_1(\boldsymbol{r}, \boldsymbol{r}')$ and it must contain some harmonic part too, in order to satisfy the boundary conditions (12), (13). The function $g_0(\boldsymbol{r}, \boldsymbol{r}')$ will contain only this logarithmic potential (multiplied by constant F_0), but it is harmonic function in the region "0" because point $(x', z') \in L$. Using the known "mirror method" we shall suppose functions $g_0(\boldsymbol{r} - \boldsymbol{r}')$ and $g_1(\boldsymbol{r} - \boldsymbol{r}')$ in the form:

$$g_0(\boldsymbol{r}, \boldsymbol{r}') = F_0 \ln \left[(x - x')^2 + (z - z')^2\right]^{-1/2} \tag{16}$$

$$g_1(\boldsymbol{r},\boldsymbol{r}') = \ln\left[(x-x')^2+(z-z')^2\right]^{-1/2} + \\ + F_1 \ln\left[(x-x')^2+(z+z')^2\right]^{-1/2}. \tag{17}$$

One can easily find that gradients of these functions vanish for points (x,z) at large distances from the source point (x',z'), which guarantees zero values of the magnetic field intensity due to the perturbing body. Coefficients F_0 and F_1 must be determined from boundary conditions at $z=0$. The equations (12) and (13) then give:

$$F_0 = 1+F_1, \qquad F_0 = (\mu_1/\mu_0)(1-F_1),$$

which result into:

$$F_0 = \frac{2(\mu_0/\mu_1)}{1+\mu_0/\mu_1} = \frac{2}{1+\mu_1/\mu_0}, \tag{18}$$

$$F_1 = F_0 - 1 = (1-\mu_1/\mu_0)/(1+\mu_1/\mu_0). \tag{19}$$

So, the necessary Green's functions for our problem are:

$$g_0(\boldsymbol{r},\boldsymbol{r}') = F_0 \ln|\boldsymbol{r}-\boldsymbol{r}'|^{-1}, \tag{20}$$

$$g_1(\boldsymbol{r},\boldsymbol{r}') = \ln|\boldsymbol{r}-\boldsymbol{r}'|^{-1} + F_1 \ln|\boldsymbol{r}_*-\boldsymbol{r}'|^{-1}, \tag{21}$$

where $\boldsymbol{r}_* \equiv (x,-z)$ is the mirror point to the point (x,z), so it is:

$$|\boldsymbol{r}_*-\boldsymbol{r}'|^{-1} = \left[(x-x')^2+(z+z')^2\right]^{-1/2}. \tag{22}$$

Now we have prepared the Green's functions as kernels of integral solution expressed by 4a–c.

3. Algorithm for numerical calculations

In numerical calculations we can use most of the experience from solutions of the B. I. E. in more simple case *(Hvoždara, 1983, 1986)*, where the Green's function was only $\ln|\boldsymbol{r}-\boldsymbol{r}'|^{-1}$. The key step for numerical solution of the B. I. E. is necessary to have the formulae for the normal derivatives of both terms in $g_1(\boldsymbol{r},\boldsymbol{r}')$ given by (17). For the first part we have expression given by (9) and we need to integrate it along the elementary segments Δs_ℓ, which compose at collocation method of solution of B. I. E. the whole contour L. According to the explanations from *(Hvoždara, 1983)* we have:

$$\int\limits_{\Delta s_\ell} \frac{\partial}{\partial n'} \ln\left[(x-x')^2+(z-z')^2\right]^{-1/2} = \int\limits_{\Delta s_\ell} \frac{\boldsymbol{n}'\cdot(\boldsymbol{r}-\boldsymbol{r}')}{|\boldsymbol{r}-\boldsymbol{r}'|^2}\,\mathrm{d}\,\ell' = \omega(P_j, Q_\ell), \quad (23)$$

where $\omega(P_j, Q_\ell)$ is the plane angle of view subtended from the point P_j onto segment Δs_ℓ with the central point Q_ℓ and outer normal $\boldsymbol{n}'$, while this angle must be multiplied by the signum of the scalar product of vectors $\boldsymbol{n}'$ and $(\boldsymbol{r}-\boldsymbol{r}')$. By means of cosine theorem applied to the triangle scheme in Fig. 2 there is

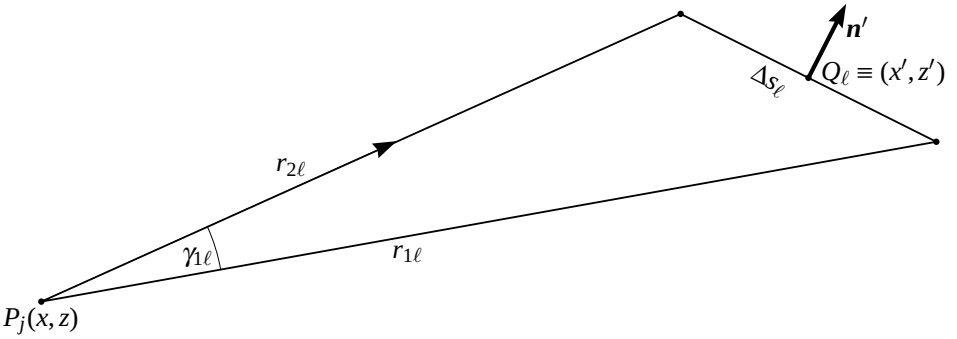

Fig. 2. Explanation sketch of the calculation of the plane angle of view onto a linear segment.

$$\Delta s_\ell = \left[r_{1\ell}^2 + r_{2\ell}^2 - 2r_{1\ell}r_{2\ell}\cos\gamma_{j\ell}\right]^{1/2},$$

so the value of cosine for $\gamma_{j\ell}$ is

$$\cos\gamma_{j\ell} = \left[r_{1\ell}^2 + r_{2\ell}^2 - (\Delta s_\ell)^2\right]/2r_{1\ell}r_{2\ell}, \quad (24)$$

and for $\omega(P_j, Q_\ell)$ we have:

$$\omega(P_j, Q_\ell) = \gamma_{j\ell}\,\mathrm{sign}\left[\boldsymbol{n}'\cdot(\boldsymbol{r}-\boldsymbol{r}')\right]. \quad (25)$$

For the normal derivative of the second logarithmic part in $g_1(\boldsymbol{r}, \boldsymbol{r}')$ we use similar treatment, so we can write

$$\omega^*(P_j^*, Q_\ell) = \int\limits_{\Delta s_\ell} \frac{\boldsymbol{n}'\cdot(\boldsymbol{r}_{*j}-\boldsymbol{r}')}{|\boldsymbol{r}_{*j}-\boldsymbol{r}'|^2}\,\mathrm{d}\,\ell' = \int\limits_{\Delta s_\ell} \frac{n'_x(x_j-x') + n'_z(-z_j-z')}{(x_j-x')^2+(z_j+z')^2}\,\mathrm{d}\,\ell' =$$

$$= \gamma^*_{j\ell}\cdot\mathrm{sign}\left[\boldsymbol{n}'\cdot(\boldsymbol{r}_*-\boldsymbol{r}')\right]. \quad (26)$$

The geometrical sense of the angle $\gamma^*_{j\ell}$ is identical with the plane angle of view from the point $P^* \equiv (x, -z)$ onto segment Δs_ℓ around the point $Q_\ell \in L$. As it was mentioned above, for the collocation solution of the B. I. E. we divide each segment T_k into smaller pieces of equal length Δs_ℓ, their number let be m_k and the sum of m_k is equal M. For practical use we suggest $5 \leq m_k \leq 20$, according to the length T_k. So we must keep

$$\sum_{k=1}^{N} m_k = M, \tag{27}$$

where the total number of Δs_ℓ should be 50–100 according to total length L. The numbers m_k must be optional for purposes of the accuracy tests of solution of the B. I. E. (8). As we already mentioned, this method supposes the piecewise constant approximation of the unknown function $f(P)$ - its value is equal to the centred one $f(Q_\ell)$ in the whole segment $\Delta \ell_j$. Then we can write the B. I. E. (8) in the form

$$f(P_j) = 2\beta\,[V_1(P_j) - v_0] + \frac{\beta}{\pi} \sum_{\ell=1}^{M}{}^{*} f(Q_\ell)\, u(P_j, Q_\ell), \tag{28}$$

where the asterisk over the summation sign denotes omission of the contribution from $\ln |\boldsymbol{r} - \boldsymbol{r}'|^{-1}$ on the segment Δs_ℓ, where $P_j \equiv Q_\ell$, in accordance with the rules of principal value integration. In a view to the formula (23) it also reflects that in this situation the normal vector $\boldsymbol{n}'$ is perpendicular to the vector $(\boldsymbol{r}_j - \boldsymbol{r}')$ for the points $Q(\boldsymbol{r}') \in T_k$, $P(\boldsymbol{r}) \in T_k$, which simplifies numerical calculations, because there will not occur any singular terms. The weighting factor $u(P_j, Q_\ell)$ are denoted by the integral:

$$u(P_j, Q_\ell) = \int\limits_{\Delta s_\ell} \frac{\partial}{\partial n'} g_1(\boldsymbol{r}, \boldsymbol{r}')\, \mathrm{d}\,\ell', \tag{29}$$

where are included both angles of view $\gamma_{j\ell}$, $\gamma^*_{j\ell}$ onto the segment Δs_ℓ. The equation (28) tells us that into value $f(P_j)$ there are incorporated contributions from all $f(Q_\ell)$ (with some weighting factors) at segments Δs_ℓ forming L.

The geometrical relations, which occur at numerical calculations we illustrate on the example of segment T_3 depicted in Fig. 3. This segment connects points A_3 and A_4 where we generated 6 subsegments (pieces) with

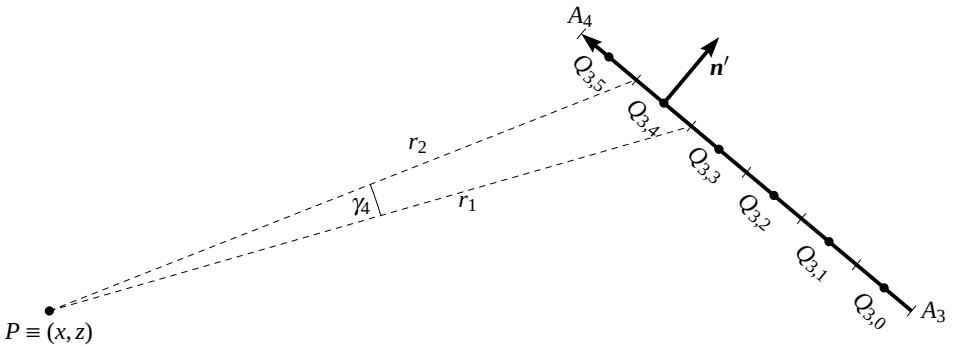

Fig. 3. Subdivision of the vector T_3 into five subsegments.

centres $Q_{3,0} - Q_{3,5}$. The normal vector for the whole segment T_3 is $\boldsymbol{n}'_3$ and its Carthesian components we calculate from equations $\boldsymbol{n}'_3 \times \boldsymbol{T}_3/T_3 = 1$ and $\boldsymbol{n}'_3 \cdot \boldsymbol{T}_3 = 0$, which reflect the mutual orthogonality of vectors $\boldsymbol{T}_3$ and $\boldsymbol{n}'_3$. Then it is clear that $\boldsymbol{n}'_3$ is constant unit vector for the whole segment T_3, its components can be calculated from the co-ordinates of the terminal points A_3, A_4. The length of the vector $\boldsymbol{T}_3 = \boldsymbol{A}_3\boldsymbol{A}_4$ is given by the formula (1):

$$T_3 = \left[(x'_4 - x'_3)^2 + (z'_4 - z'_3)^2\right]^{1/2}, \tag{30}$$

because the vector $\boldsymbol{T}_3$ is:

$$\boldsymbol{T}_3 = (x'_4 - x'_3)\boldsymbol{e}_x + (z'_4 - z'_3)\boldsymbol{e}_z. \tag{31}$$

As we already noted there must hold vector relations: $\boldsymbol{n}'_3 \times \boldsymbol{T}_3/T_3 = 1$ and $\boldsymbol{n}'_3 \cdot \boldsymbol{T}_3 = 0$, since the angle between $\boldsymbol{n}'_3$ and $\boldsymbol{T}_3$ is $\pi/2$. Then we can easily find Carthesian components of $\boldsymbol{n}'_3$:

$$n'_x = -\frac{z'_4 - z'_3}{T_3}, \qquad n'_z = +\frac{x'_4 - x'_3}{T_3}. \tag{32}$$

Similar treatment we apply for all segments $\boldsymbol{T}_k$. We see, that as soon as we have defined contour polygon L of the perturbing body, we can easily determine normal vectors on all segments $\boldsymbol{T}_k$. These values we must use for calculations of weighting factors for discretized B. I. E. On the basis of treatment given in *Hvoždara (1983)* we know that the most important term in the weighting factor is $\omega(P_j, Q_\ell) = \gamma_{\ell j} \cdot \mathrm{sign}\,[\boldsymbol{n}'_\ell \cdot (\boldsymbol{r}_j - \boldsymbol{r}'_\ell)]$. For the case

of convex contour line L as shown in Fig. 1 all these values will be negative or zero, because $\mathrm{sign}[\boldsymbol{n}'_\ell \cdot (\boldsymbol{r}'_j - \boldsymbol{r}'_\ell)] < 0$, since angles between $\boldsymbol{n}'_\ell$ and $(\boldsymbol{r}'_j - \boldsymbol{r}'_\ell)$ are obtuse, the zero value is for the case when $P(\boldsymbol{r}_j)$ an $Q(\boldsymbol{r}_\ell)$ belong to the same straight line segment.

There is also necessary to note, that for contour integral of plane angle of view there holds true a very important formula – the Gaussian integral *(Tichonov and Samarskij, 1966)*:

$$\oint_L \frac{\boldsymbol{n}' \cdot (\boldsymbol{r} - \boldsymbol{r}')}{|\boldsymbol{r} - \boldsymbol{r}'|^2} \, \mathrm{d}\, \ell' = \begin{cases} 0, \text{for } P(\boldsymbol{r}) \in \mathrm{Ext}(L) \\ -\pi, \text{for } P(\boldsymbol{r}) \in L \\ -2\pi, \text{for } P(\boldsymbol{r}) \in \mathrm{Int}(L)\,. \end{cases} \tag{33}$$

The case $P(\boldsymbol{r}) \in L$ of this formula provides us very good check of accuracy of calculation of $\omega(P_j, Q_\ell)$, because at calculation of weighting factors of the B. I. E. (9) we must attain the control value:

$$\sum_{\ell=1}^{M} \omega(P_j, Q_\ell) \doteq -\pi, \tag{34}$$

with accuracy better than 1%, otherwise we did not introduce fine enough subdivision of the contour L, or in our program code we have another errors. The second term in $g_1(\boldsymbol{r} - \boldsymbol{r}')$ is function $\ln |\boldsymbol{r}_* - \boldsymbol{r}'|^{-1}$ which is harmonic function and from the Gaussian integral (33) follows its check value:

$$\sum_{\ell=1}^{M} \omega^*(P^*_j, Q_\ell) \doteq 0, \tag{35}$$

because for $\ln |\boldsymbol{r}_* - \boldsymbol{r}'|^{-1}$ the point of view $P^* \equiv (x, -z)$ lies in $\mathrm{Ext}(L)$. The discretized form of B. I. E. (9) can be written in a classical system of M linear equations:

$$\sum_{\ell=1}^{M} C_{\ell j} \cdot X_\ell = b_j, \qquad j = 1, 2, \ldots, M, \tag{36}$$

$$b_j = 2\beta[V_1(P_j) - v_0], \tag{37}$$

are elements of the right side vector (they represent the values of the exciting potentials) on elements $\Delta\ell_j$. Elements of the matrix of the system (36) are:

$$C_{\ell j} = \delta_{\ell j} - \beta\pi^{-1} \cdot u(P_j, Q_\ell), \tag{38}$$

where $\delta_{\ell j}$ is Kronecker's symbol ($\delta_{\ell j} = 1$ if $\ell = j$ and $\delta_{\ell j} = 0$ for $\ell \neq j$). Values of (till) unknown function $f(Q)$ collocated for centres of intervals Δs_ℓ are represented in elements of solution vector $X_\ell = f(Q_\ell)$. The system of equations (36) expresses that in each value $f(Q_j)$ are included contributions from all M elements of the contour polygon. It is necessary to stress that subdivision onto elements Δs_ℓ must be dense enough, because the theory of potential requires the continuity of $f(Q)$ along L, which means that the changes of neighbouring values $f(Q_\ell)$ should not be greater than 5–10%. If this condition of "quasi continuity" is violated on some segment T_k we must increase the number of subdivisions. Another check of accuracy is the comparison of values of $f(Q_\ell)$ for gradually increased number of subdivision (M), e.g. $M = 50$, 80, 120, 160 which is easily possible to perform on contemporary PC-computers. As soon as the solution of (36) is performed with satisfactory accuracy, we can calculate the approximations of potentials by means of formulae (4a–c). From the practical needs there are more necessary values of the intensity, especially of its anomalous part.

4. Calculation of the intensity of magnetic field outside of perturbing body

According to the formula (2) there is necessary to calculate gradients of the integral parts of potentials (4a–c) and derivatives we must perform with respect to the co-ordinates x, z (undashed) of the point P. This derivation must be applied at first to the kernel function

$$w(P, Q) = \frac{\partial}{\partial n'} \ln \frac{1}{|\boldsymbol{r} - \boldsymbol{r}'|} = \frac{n'_x(x - x') + n'_z(z - z')}{|\boldsymbol{r} - \boldsymbol{r}'|^2}. \tag{39}$$

We can easily find that there is

$$\frac{\partial}{\partial x} w(P, Q) = \frac{n'_x}{|\boldsymbol{r} - \boldsymbol{r}'|^2} \left[1 - \frac{2(x - x')^2}{|\boldsymbol{r} - \boldsymbol{r}'|^2}\right] - \frac{2n'_z(x - x')(z - z')}{|\boldsymbol{r} - \boldsymbol{r}'|^4}, \tag{40}$$

$$\frac{\partial}{\partial z} w(P, Q) = \frac{-2n'_x(x - x')(z - z')}{|\boldsymbol{r} - \boldsymbol{r}'|^4} + \frac{n'_z}{|\boldsymbol{r} - \boldsymbol{r}'|^2} \left[1 - \frac{2(z - z')^2}{|\boldsymbol{r} - \boldsymbol{r}'|^2}\right]. \tag{41}$$

These weighting functions must be used for the calculation of the components of magnetic field in region "0", where the Green's function is $F_0 \ln|\boldsymbol{r}-\boldsymbol{r}'|^{-1}$. We were not successful to find some reliable analytical formula of integration of expressions (40), (41) for the general slope of Δs_ℓ, so we satisfied with difference approximations of derivatives (negative), calculated from values of $U_0^*(P)$, in the dense enough network of points x, z outside of the perturbing body. In the points very distant from the perturbing body we can use the collocated approximations of the intensity. As a measure of distance we can use the length $D \approx 3\sqrt{S}$, from the centre of the body, S is the size of $\mathrm{Int}(S)$. Then we have:

$$\Delta H_{0x}^*(x,z) \doteq -\frac{F_0}{2\pi}\sum_{\ell=1}^{M} f(Q_\ell)\left\{\frac{n'_{x\ell}}{|\boldsymbol{r}-\boldsymbol{r}'_\ell|^2}\left[1-\frac{2(x-x'_\ell)^2}{|\boldsymbol{r}-\boldsymbol{r}'_\ell|^2}\right]-\right.$$

$$\left.-\frac{2n'_{z\ell}(x-x'_\ell)(z-z'_\ell)}{|\boldsymbol{r}-\boldsymbol{r}'_\ell|^4}\right\}\Delta s'_\ell, \tag{42}$$

where (x, z) are co-ordinates of the calculation point P in the region "0" at the distance greater than D.

$$\Delta H_{0z}^*(x,z) \doteq -\frac{F_0}{2\pi}\sum_{\ell=1}^{M} f(Q_\ell)\left\{\frac{n'_{z\ell}}{|\boldsymbol{r}-\boldsymbol{r}'_\ell|^2}\left[1-\frac{2(z-z'_\ell)^2}{|\boldsymbol{r}-\boldsymbol{r}'|^2}\right]-\right.$$

$$\left.-\frac{2n'_{x\ell}(x-x'_\ell)(z-z'_\ell)}{|\boldsymbol{r}-\boldsymbol{r}'_\ell|^2}\right\}\Delta s'_\ell. \tag{43}$$

In these formulae we substitute $|\boldsymbol{r}-\boldsymbol{r}'_\ell|^2 = (x-x'_\ell)^2+(z-z'_\ell)^2$.

In the region "1" outside of perturbing body we have Green's function $g_1(\boldsymbol{r},\boldsymbol{r}') = \ln|\boldsymbol{r}-\boldsymbol{r}'|^{-1} + F_1 \ln|\boldsymbol{r}_*-\boldsymbol{r}'|^{-1}$, so the expressions of ΔH_{1x} and ΔH_{1z} will be more complicated in comparison to (42) and (43). For this reason we write their abbreviated expressions:

$$\Delta H_{1x}^*(x,z) = \frac{-1}{2\pi}\sum_{\ell=1}^{M} f(Q_\ell)\frac{\partial}{\partial x}\left[\frac{\partial}{\partial n'}\, g_1(\boldsymbol{r},\boldsymbol{r}')\right]\Delta s'_\ell\,, \tag{44}$$

$$\Delta H_{1z}^*(x,z) = \frac{-1}{2\pi}\sum_{\ell=1}^{M} f(Q_\ell)\frac{\partial}{\partial z}\left[\frac{\partial}{\partial n'}\, g_1(\boldsymbol{r},\boldsymbol{r}')\right]\Delta s'_\ell\,, \tag{45}$$

while the more detailed expressions of these derivatives are similar to (42) and (43).

5. Numerical calculation and discussion

Our numerical calculations we have performed for the calculation of the anomalous magnetic fields $\Delta \boldsymbol{H}_{0,1}$ for 2D bodies of two polygonal types:
a) unequilateral 10 vertices polygon,
b) the trapezoid (the valley or gallery).
The calculations were programed in the Fortran77 language. The perturbing potential was calculated for 5–8 levels $z_m (m = 1, \ldots, 8)$ and on each level there was calculated potential $U_0^*(x, z)$ or $U_1^*(x, z)$ with constant step Δx, i.e. for $x_n = x_0 + n \cdot \Delta x + \Delta x/2,\ n = 0, J_{max}$. In a view of better accuracy the potential was calculated for the two neighbouring levels to $z = z_m$, i.e. for the level $z_m - \Delta z$ and $z_m + \Delta z$. Then we have necessary approximations for x and z derivatives according to the rules of difference calculus:

$$(\partial \Psi/\partial x) \approx (1/2)\,[\Psi(x + \Delta x/2, z - \Delta z) - \Psi(x - \Delta x/2, z - \Delta z) + \\ + \Psi(x + \Delta x/2, z + \Delta z) - \Psi(x - \Delta x/2, z + \Delta z)]\,/\Delta x\,, \tag{46}$$

$$(\partial \Psi/\partial z) \approx (1/4)\,[\Psi(x - \Delta x/2, z + \Delta z) - \Psi(x - \Delta x/2, z - \Delta z) + \\ + \Psi(x + \Delta x/2, z + \Delta z) - \Psi(x + \Delta x/2, z - \Delta z)]\,/\Delta z\,. \tag{47}$$

The grid of calculation points around the point x, z is sketched in the Fig. 4. It is clear that steps Δx and Δz must be adopted to the horizontal (L_x) and vertical (L_z) dimensions of the body: $\Delta x \leq L_x/10$ and $\Delta z \leq L_z/10$. By means of application of these difference formulae onto anomalous potentials $U_0^*(x, z)$ or $U_1(x, z)$, we calculate components of anomalous intensity $\Delta H_{0,1}$ and by addition of the unperturbed magnetic field and multiplication with permeability we obtain the resulting magnetic induction

$$\boldsymbol{B}_{0,1} = \mu_{0,1} \boldsymbol{H}_{0,1}\,. \tag{48}$$

Then we calculate the values of the total magnetic field

$$\Delta T = |\boldsymbol{B}_{0,1}| - |\boldsymbol{B}_n|\,, \tag{49}$$

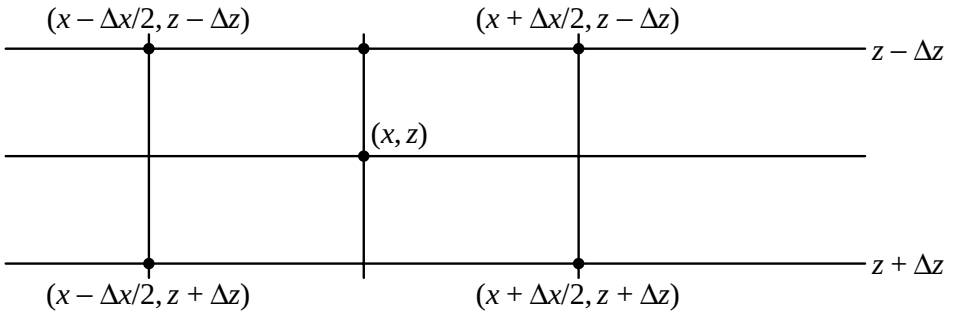

Fig. 4. Rectangular grid pattern for approximative calculations of x, z derivatives of magnetic potential.

as well as the anomaly of inclination

$$\Delta I = \operatorname{arctg}(B_z/B_x) - I_0\,, \tag{50}$$

where $\boldsymbol{B}_n$ is the vector of normal induction and I_0 its inclination. In our numerical calculations we adopted the susceptibility of rocks in lava field (halfspace "1") to be $\kappa_1 = 0.01$ SI and two values of susceptibility κ_2 for perturbing body $\kappa_2 = 0.05$ SI (increased susceptibility) or $\kappa_2 = 0.001$ SI (low susceptibility) so we have $\mu_1 = \mu_0(1+\kappa_1)$, $\mu_T = \mu_0(1+\kappa_2)$. The results of the numerical calculations we plotted in curves of ΔT and ΔI, together with the cross-sections of the body. The dimensions of the body "2" were normed to lengths d^*, h^* (given in meters in figures), the horizontal co-ordinate x was normed to d^*, while $h^* = \frac{1}{2}\,[(z_k)_{\max} + (z_k)_{\min}]$, $d^* = \operatorname{Max}(h^*, \overline{x})$, where $\overline{x} = (x_k)_{\max} - (x_k)_{\min}$. The form of the body was normed to the common scale d^*, in order to have the undeformed shape of polygon L.

As a first model we calculated the effect of the 2D body with circumference given as 10-corner polygon depicted in the bottom of Figs 5a, b. The lower boundary of this polygon is in the depth 1200 m, the span in x direction is 1800 m. The broken top boundary of the polygon lies in depths 300 to 400 m. The magnetic effect ΔT and ΔI we calculated for levels $z/h^* = -0.08, -0.04, 0.0, 0.04, 0.08, 0.12$, which are identical with levels $z = -60, -30, 0, 30, 60, 90$ m. The profile curves ΔT plotted in Fig. 5a quite expressively reflect the relief of the upper boundary, while the values of ΔT reach about 400 nT in region $x < 0$ (incident part), where the anomalous magnetic field increases the primary field. From this maximum

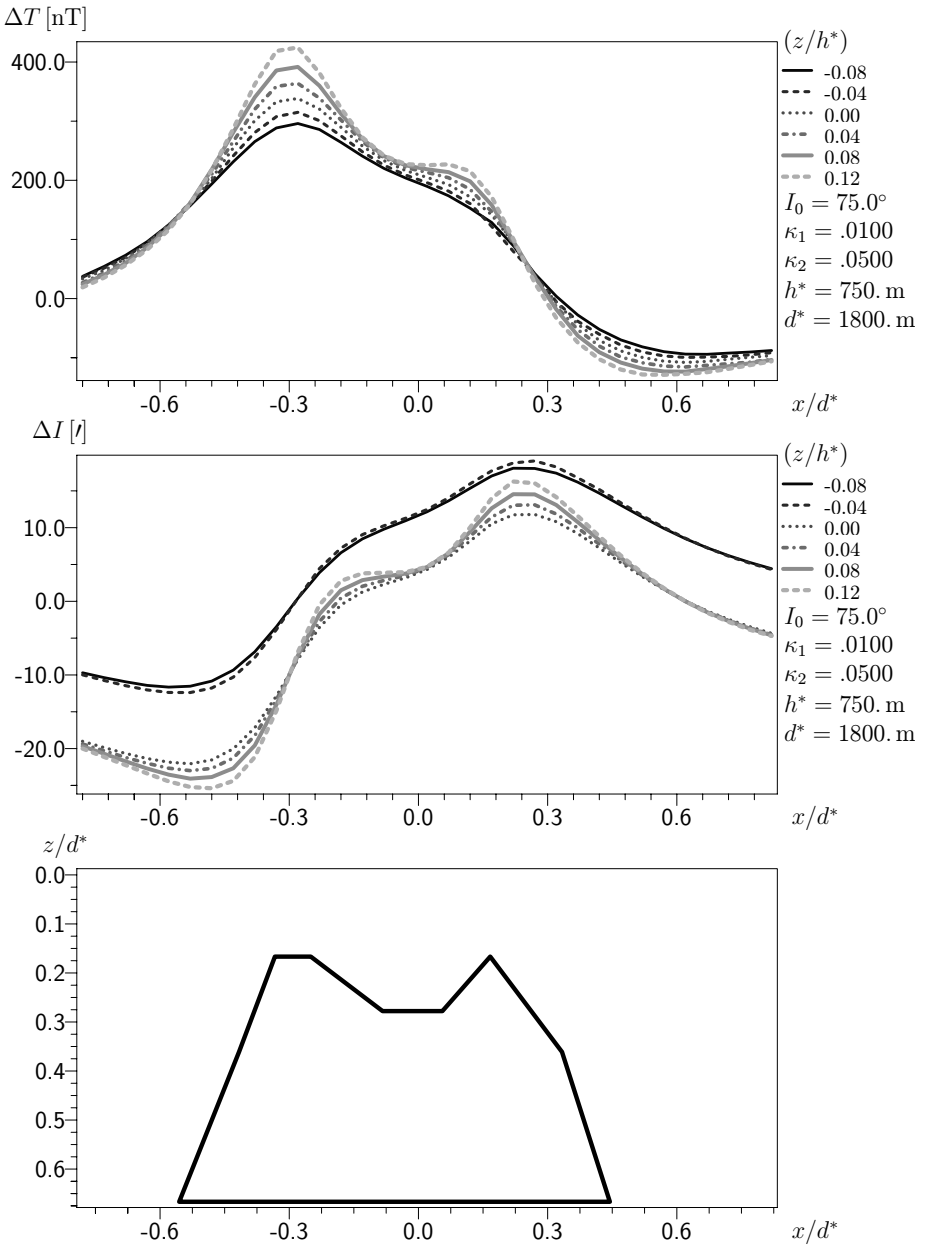

Fig. 5a. Profile anomalies of ΔT and ΔI for the polygonal (10-vertex) body with increased permeability $\mu_T = \mu_0(1+\kappa_2)$. The permeability of surrounding halfspace is $\mu_1 = \mu_0(1+\kappa_1)$.

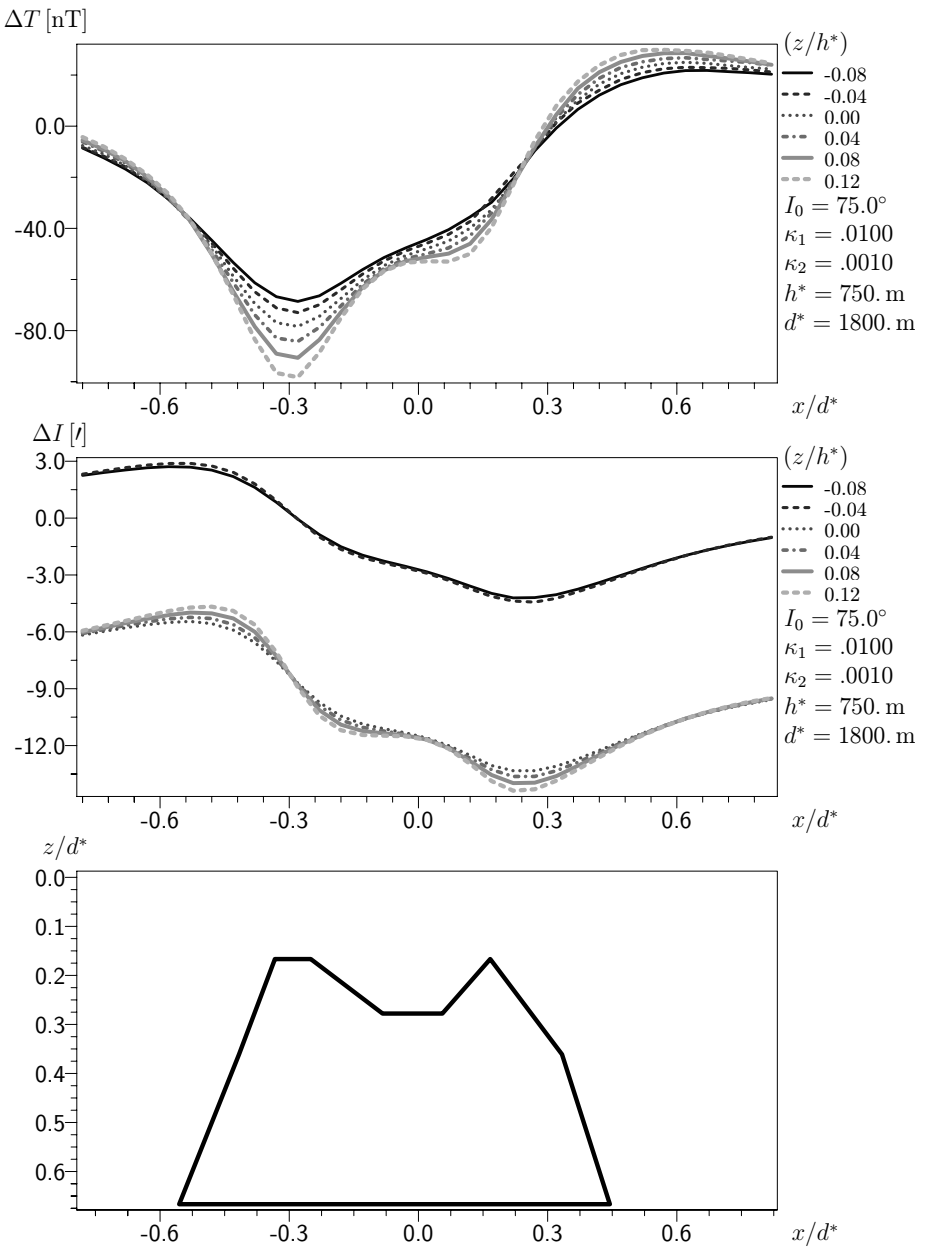

Fig. 5b. The same as Fig. 5a, but the body has decreased permeability.

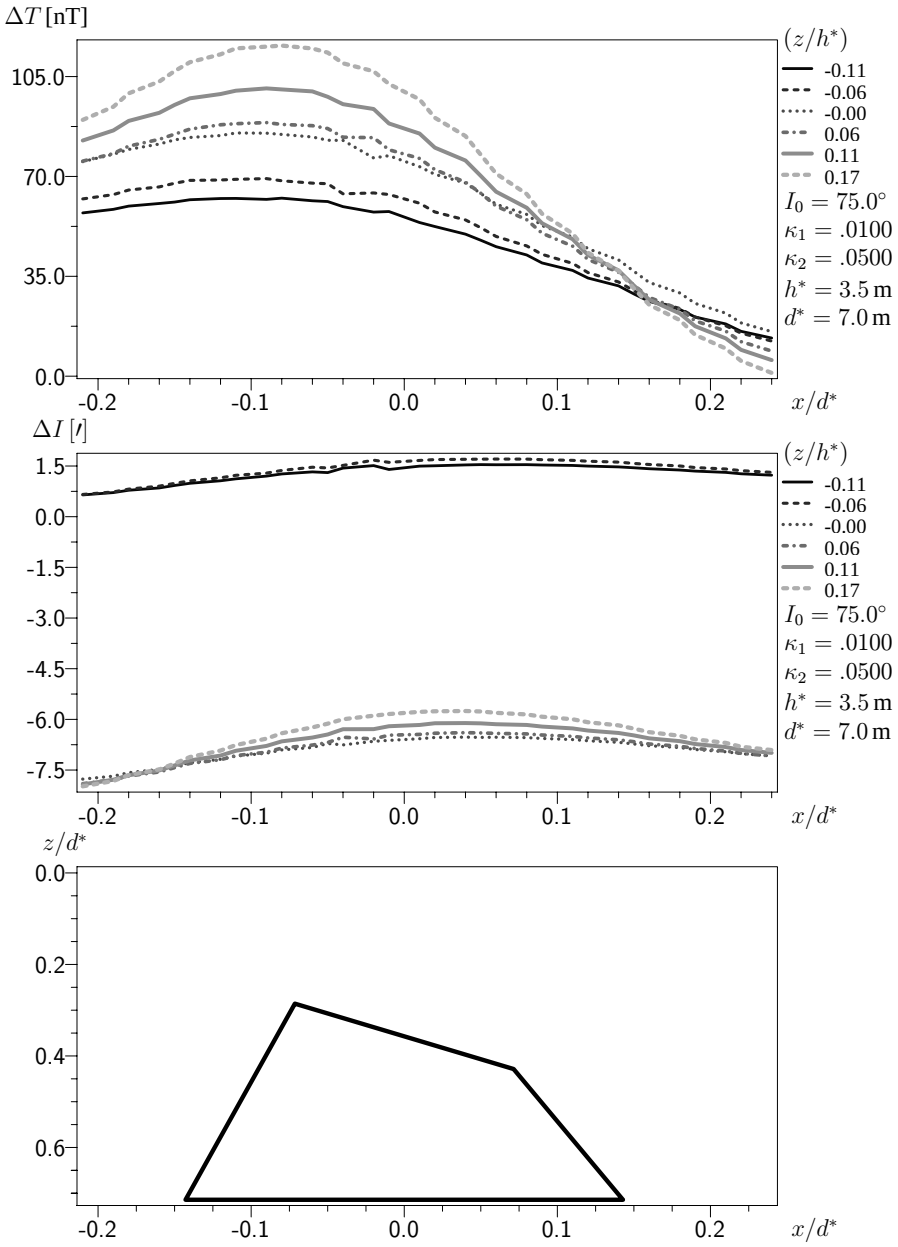

Fig. 6a. Profile anomalies of ΔT and ΔI for the trapezoidal body with increased permeability $\mu_T = \mu_0(1 + \kappa_2)$. The permeability of surrounding halfspace is $\mu_1 = \mu_0(1 + \kappa_1)$.

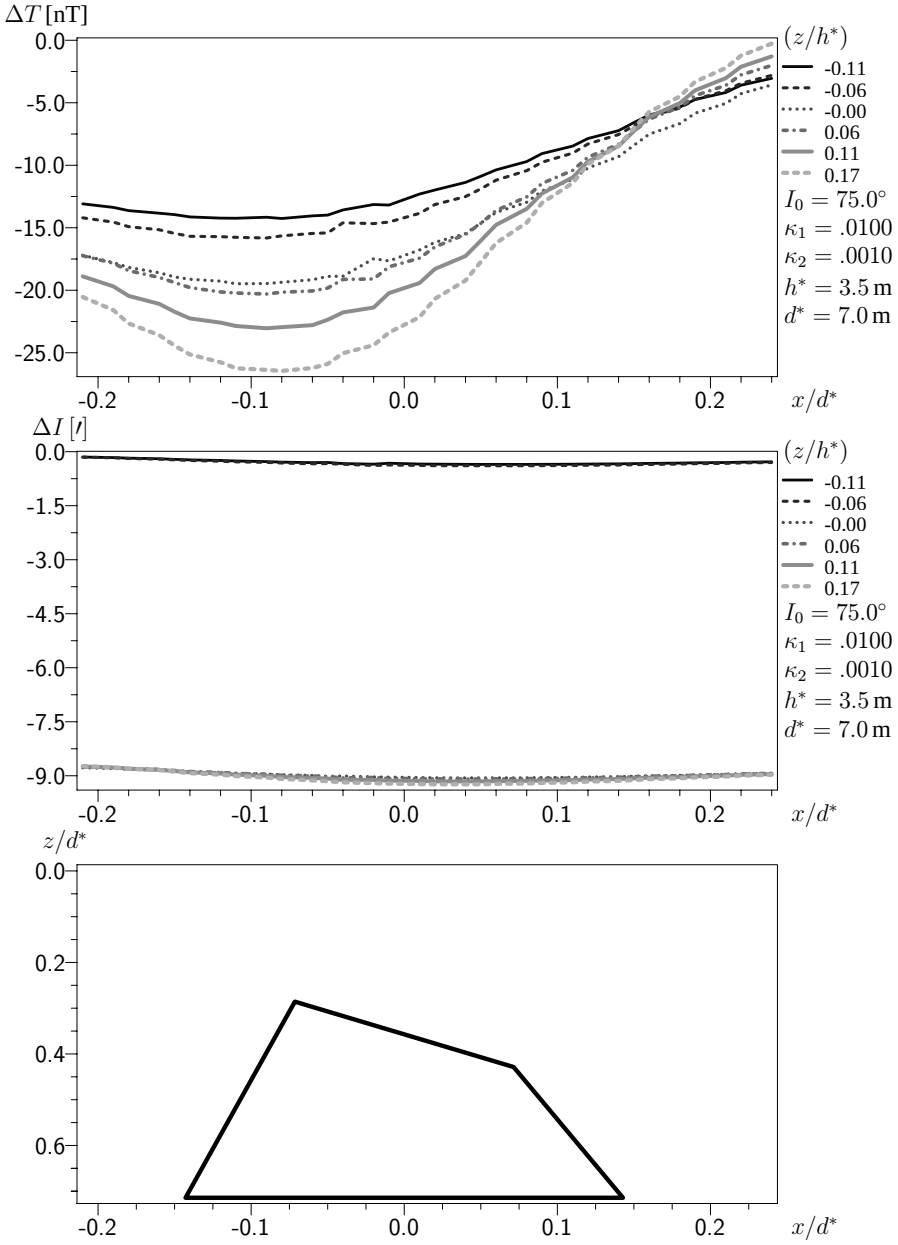

Fig. 6b. The same as Fig. 6a, but the body has decreased permeability (e.g. non-magnetic gallery).

values ΔT decrease to minimal values in the "leeward" side $\Delta T \approx -50\,\mathrm{nT}$, which is due to the opposite direction of the perturbing magnetic field to the normal one. The Fig. 5b shows the opposite anomalies for the prism with low susceptibility $\kappa_2 = 0.001$. The course of curves is nearly mirrored in comparison to the curves in Fig. 5a, but their extremes are lower. These general properties of magnetic anomalies ΔT above the 2D prism are known e.g. *(Logachev and Zacharov, 1979; Telford et al., 1976)*, but our results for more complicated cross-sections explain some irregularities due to the non-planar shape of L, namely when they are closer to the surface. Similar calculations we performed for trapezoidal 2D body, located more close to the surface, results are presented in Figs 6a, b.

This trapezoidal model we chose as the general 4-corner polygon, situated near the surface of the earth, with the dimensions of few meters. The curves in Fig. 6a represent the effect of shallow magnetic intrusion, while Fig. 6b approximates the effect of a non-magnetic cavity, e.g. gallery. We can see that this shallow body creates magnetic anomalies of few nanoTeslas, which are measurable by the proton magnetometer.

Very interesting feature of all inclination anomalies (about ± 20 angle minutes) given in Figs 5–6 is the shift of this curves in region $z < 0$ (over halfspace) as compared with the curves ΔI inside the halfspace. The reason of this effect lies in (small) higher susceptibility of the halfspace $\kappa_1 = 0.01\,\mathrm{SI}$ and the higher or lower susceptibility κ_2 gives further anomaly.

Acknowledgments. The authors are grateful to the Slovak Grant Agency VEGA (grant No. 2/4042/24) for the partial support of this work.

References

Grant F. S., West G. F., 1965: Interpretation Theory in Applied Geophysics. McGraw-Hill Book Comp., New York.

Hvoždara M., 1983: Solution of the direct problem of magnetometry with the aid of the potential of a dipole layer. Contr. Geophys. Ins. SAS, **14**, 23–46.

Hvož dara M., 1986: Anomaly of the telluric field due to a two-dimensional disturbing body in a two-layered Earth. Contr. Geophys. Inst. SAS, **16**, 33–48.

Hvoždara M., Kaplíková A., 2005: Magnetic anomaly due to magnetic halfspace with buried cylindrical perturbing body. Contr. Geophys. Geod., **35**, 2, 127–139.

Logachev A. A., Zacharov V. P., 1979: Magnetometry. Nedra, Leningrad (in Russian),

Moon P., Spencer D. E., 1971: Field theory handbook. Springer-Verlag, Berlin.

Stratton J. A., 1941: Electromagnetic theory. McGraw-Hill, New York.

Tichonov A. N., Samarskij A. A., 1966: Equations of Mathematical Physics. Nauka, Moscow (in Russian).

Telford W. M., Geldart L. P., Sheriff R. E., Keys D. A., 1976: Applied geophysics. Cambridge University Press.